Direct binding of NuMA to tubulin is mediated by a novel sequence motif in the tail domain that bundles and stabilizes microtubules

Laurence Haren and Andreas Merdes*

Wellcome Trust Centre for Cell Biology, Institute of Cell and Molecular Biology, University of Edinburgh, King's Buildings, Edinburgh, EH9 3JR, UK
*Author for correspondence (e-mail: a.merdes@ed.ac.uk)

Accepted 6 February 2002
Journal of Cell Science 115, 1815-1824 (2002) © The Company of Biologists Ltd

Summary

In mitosis, NuMA localises to spindle poles where it contributes to the formation and maintenance of focussed microtubule arrays. Previous work has shown that NuMA is transported to the poles by dynein and dynactin. So far, it is unclear how NuMA accumulates at the spindle poles following transport and how it remains associated throughout mitosis. We show here that NuMA can bind to microtubules independently of dynein/dynactin. We characterise a 100-residue domain located within the C-terminal tail of NuMA that mediates a direct interaction with tubulin in vitro and that is necessary for NuMA association with tubulin in vivo. Moreover, this domain induces bundling and stabilisation of microtubules when expressed in cultured cells and leads to formation of abnormal mitotic spindles with increased microtubule asters or multiple poles. Our results suggest that NuMA organises the poles by stable crosslinking of the microtubule fibers.

Key words: Spindle pole, Microtubule-associated protein, Mitosis

Introduction

During cell division, the microtubule network is transformed into a spindle apparatus that separates chromosome pairs and transports them to opposite poles. The functionality of these spindle poles depends on focussed arrays of microtubule minus-ends, in most animal cells anchored in a matrix of electron-dense material surrounding the centrosomes. But even cell types that don't contain centrosomes, such as oocytes in many animal species, are capable of organizing intact spindle poles. This is done with the help of structural and motor proteins that accumulate at microtubule minus-ends during spindle formation (for reviews, see Merdes and Cleveland, 1997; Compton, 1998). In *Drosophila*, a set of pole-forming proteins has been characterized, including Asp (Avides and Glover, 1999; Wakefield et al., 2001), D-TACC (Gergely et al., 2000b; Cullen and Ohkura, 2001; Lee et al., 2001), the microtubule-associated protein Msps (Cullen et al., 1999), and the minus-end directed motor protein Ncd (Matthies et al., 1996). There are homologues of several of these proteins in vertebrates that fulfil similar roles: a protein family related to D-TACC has been described (Gergely et al., 2000a), the protein Msps is a homologue of ch-TOGp and XMAP 215 (Charrasse et al., 1998; Dionne et al., 2000), and the kinesin-related protein Ncd is very similar to the human motor protein hSET and the protein CHO2 in rodents (Kuriyama et al., 1995; Mountain et al., 1999).

Other spindle pole proteins, NuMA and TPX2, have been identified only in vertebrates (Compton et al., 1992; Yang et al., 1992; Wittmann et al., 2000). Both NuMA and TPX2 show a cell-cycle-dependent localization: they are nuclear during interphase, and re-localize to the spindle poles in mitosis. Despite varying protein compositions, the mechanisms for spindle pole organization in vertebrates and *Drosophila* seem to share striking similarities: NuMA has been shown to associate with the minus-end directed motor dynein and the activator dynactin and is transported towards the poles at early stages of spindle formation (Merdes et al., 1996; Merdes et al., 2000). By attaching to parallel microtubules in the spindle, the moving NuMA complex can focus them in a zipper-like fashion. By analogy, it was proposed that the *Drosophila* protein Msps is transported polewards by Ncd, where it has a stabilizing effect on the microtubule ends (Cullen and Ohkura, 2001). Whereas Msps is anchored to the spindle poles by D-TACC, the mechanisms that retain NuMA at the poles are less clear: Although the association of NuMA with dynein and dynactin in a multi-protein complex can explain the transport of NuMA along spindle fibres and the process of microtubule focussing, the question remains how NuMA is able to attach and accumulate at the poles, and why the protein isn't falling off the microtubule minus-ends following transport. Previously, we suggested that NuMA might possess a direct affinity for microtubules (Merdes et al., 1996), which could provide stable crosslinking of spindle fibres once NuMA is deposited at the poles. In this report, we provide direct evidence for this model: we map and characterize a 100-residue region in the tail domain of NuMA that binds directly to tubulin, and that induces formation of microtubule bundles with an increased stability.

Materials and Methods

Binding studies in vitro

Cytostatic factor-arrested *Xenopus laevis* egg extract was prepared as described (Murray, 1991). A high speed supernatant of the extract was

prepared by centrifugation at 150,000 ***g*** for one hour. To inhibit dynein or dynactin, antibody 70.1 from Sigma (Dorset, UK) or p50/dynamitin were added as described (Merdes et al., 2000). Samples of 100 μl were incubated for 30 minutes with 1 μM taxol and 45 μg taxol-stabilized microtubules, and subsequently mixed with 700 μl BRB80 (80 mM K-PIPES, 1 mM $MgCl_2$, 1 mM EGTA, pH 6.8) supplemented with 0.1% Triton X-100, 1 mM dithiothreitol, 5 mM EGTA, leupeptin, pepstatin, chymostatin and cytochalasin B. The mixture was loaded onto a 750 μl cushion of 25% glycerol in the same buffer and centrifuged in a Beckman TLS55 rotor for 15 minutes at 35,000 ***g*** and 20°C. Pellets were resuspended in 150 μl buffer and one-tenth of each volume was separated on a 5% SDS polyacrylamide gel. Phosphatase treatment of 1 μl concentrated low speed egg extract was performed for 30 minutes at 30°C using 300 units of lambda protein phosphatase (New England Biolabs, Hertfordshire, UK) in a total volume of 20 μl, containing phosphatase buffer and 2 mM $MnCl_2$ supplied from the manufacturer. Lambda phosphatase was inhibited with 50 mM EDTA or 50 mM sodium fluoride, according to the manufacturer's instructions. Alternatively, microtubule pellets of taxol-treated low speed extracts were resuspended in phosphatase buffer containing 2 mM $MnCl_2$, and one-quarter of this material was treated with 500 units of lambda phosphatase in a volume of 50 μl. NuMA was analyzed on immunoblots, using affinity purified antibody against a NuMA tail peptide (Merdes et al., 1996).

Hexa-histidine tagged bacterial fusion proteins of *Xenopus* NuMA tail and rod fragments were prepared as described (Merdes et al., 1996). A hexa-histidine tagged fusion protein of the *Xenopus* NuMA head domain was expressed using pRSET-C (Invitrogen, San Diego, CA), in which *Xenopus* NuMA nucleotides 196 to 885 were cloned at *Bam*HI and *Eco*RI sites, using PCR products of previously identified library clones (Merdes et al., 1996). A vector encoding hexa-histidine tagged αSNAP (Whiteheart et al., 1993) was obtained from C. Rabouille, University of Edinburgh. All fusion proteins were solubilized from bacteria in 8 M urea, 50 mM sodium phosphate, pH 7.6, purified over Ni-agarose (Qiagen, Hilden, Germany), and 50 μg of each were precipitated with 1.7 volumes of saturated ammonium sulfate. The proteins were solubilized in a total volume of 30 μl containing 23 μg of phosphocellulose-purified tubulin in BRB80. Following 1 hour incubation at room temperature, samples were diluted with 100 μl of cytoskeleton buffer (0.1 M NaCl, 0.3 M sucrose, 10 mM PIPES, 3 mM $MgCl_2$, pH 6.8), incubated for a further 10 minutes, and mixed with Ni-NTA magnetic agarose beads, pelleted from 50 μl of a 5% suspension (Qiagen). After 10 minutes of incubation on a rotator, the beads were separated from the supernatant using a magnet, and washed twice with 1 ml of cytoskeleton buffer containing 0.5 M NaCl, and twice containing additional 0.2% Triton X-100. Proteins were eluted in SDS sample buffer, separated by gel electrophoresis, and immunoblotted using either monoclonal antibody DM1α against tubulin (Sigma, Dorset, UK), or antibody against an epitope of 6×His-Gly from Invitrogen (San Diego, CA).

In a different set of experiments, NuMA fusion proteins were dialyzed against PBS, and 1.5 μg were mixed with 15 μg of previously polymerized and taxol-stabilized tubulin in a total volume of 20 μl BRB80. After 15 minutes of incubation at room temperature, the solution was carefully underlayed by 20 μl of 30% glycerol in BRB80, and centrifuged for 10 minutes at 16,000 ***g***. Supernatants and pellets were analyzed by gel electrophoresis. For the estimation of the binding constant (K_A) of NuMA tail II to tubulin, increasing amounts of NuMA tail II were used in this assay, and the material in supernatants and pellets was quantified by scanning of Coomassie-stained gels, and by quantitative immunoblotting using a phosphoimager and antibodies against tubulin or 6×His-Gly, followed by ^{125}I-labelled protein A. Analogously, microtubule binding of 0.4 μg NuMA tail II that were phosphorylated with recombinant cdc2/cyclinB (New England Biolabs, Hertfordshire, UK) and [γ-^{32}P]ATP was assayed after mixing with increasing amounts of unlabelled NuMA tail II; bound material was quantified directly from dried protein gels on a phosphoimager.

Morphological effects of NuMA tail fragments on microtubule formation with pure tubulin were studied as described (Merdes et al., 1996), with the modification that rhodamine-labelled tubulin was added to the assay. Microtubule aster formation in *Xenopus* egg extracts was studied by mixing 2.5 μg NuMA tail II or tail IIA with 10 μl of metaphase extract and incubating for 35 minutes (Merdes et al., 1996). Affinity adsorption experiments in *Xenopus* egg extracts were carried out using bacterial 6×His NuMA tail I and tail II proteins dialyzed against PBS and diluted to 0.2 mg/ml in 50 μl samples of extract. The NuMA tail proteins were recovered using 30 μl of Ni-agarose, followed by two washes in PBS and one wash in 0.2% Triton X-100 in PBS, and elution in 30 μl SDS gel sample buffer. Tubulin was identified by immunoblotting.

Transfection experiments and microscopy

HeLa cells were grown in Dulbecco's modified Eagle's medium with 10% fetal calf serum and transfected with calcium phosphate. To increase the mitotic index, a single block of 15 hours with 2 mM thymidine was used. Cells were fixed either in methanol for 20 minutes at –20°C, or with 3.7% formaldehyde in 0.1 M NaCl, 0.3 M sucrose, 10 mM PIPES, 3 mM $MgCl_2$, pH 6.8 for 10 minutes at room temperature, followed by permeabilization in 0.2% Triton X-100. Cells were incubated with PBS, 0.1% Tween, 0.5% BSA for 5 minutes, then with primary antibody [i.e. mAb1F1 anti-NuMA (Compton, 1991); anti tubulin DM1α, or anti-acetylated tubulin (both from Sigma, Dorset, UK) for 30 minutes], and with secondary antibody (Texas-Red-conjugated anti-mouse, Sigma, Dorset, UK) for 30 minutes. For actin staining, cells were incubated with TRITC-phalloidin (0.25 μM, Sigma, Dorset). After DNA staining with DAPI (2.5 μg/ml), coverslips were mounted on microscope slides with Vectashield (Vector Laboratories, Burlingame, CA) and sealed with nail polish. Conventional fluorescence microscopy was performed as described previously (Merdes et al., 2000). For electron microscopy, cells on coverslips were fixed with 1% glutaraldehyde in PBS. Cells that expressed GFP-NuMA tail II were identified by fluorescence microscopy and photographed, and coordinates of the microscope stage were recorded for following relocation. Cells were subsequently treated with 2% osmium tetroxide, dehydrated in a graded series of ethanol, and flat-embedded in Araldite CY212 (Agar Scientifc, Essex, UK). After relocation of the transfected cells, the glass coverslip surface was removed with hydrofluoric acid, and the cells were mounted on blocks of Araldite. Ultrathin sections were counterstained with lead citrate and viewed on a Philips CM120 electron microscope.

Construction of GFP-NuMA derivatives

Constructs were derived from GFP-human NuMA in the eukaryotic expression vector pCDNA3 (Merdes et al., 2000). Fragments of NuMA tail were obtained from this template by PCR, using the proofreading Pfu polymerase (Stratagene, Amsterdam, Netherlands). All primers carried the restriction sites *Not*I (5′) and *Xba*I (3′, following a STOP codon), allowing substitution of the full-length NuMA in the parental plasmid by the tail fragments. In our constructs, nucleotide positions of NuMA cDNA [GenBank Z11584 (Compton et al., 1992)] were the following: 5101-5595 for tail I, 5602-6306 for tail II, 5602-5901 for tail IIA, 5932-6306 for tail IIB. For the deletion of the nuclear localization signal in GFP-NuMA, wild-type sequence between *Eco*RV and *Xba*I in pCDNA3 GFP-NuMA was replaced by an *Eco*RV/*Eco*RI fragment of pUC19 NuMAΔNLS (Saredi et al., 1996). The deletion constructs NuMAΔtailII and ΔtailIIA+NLS were cloned by substitution of the 3′ end of NuMA in pCDNA3 GFP-NuMA with PCR products. For NuMAΔtailII, the PCR product extended from a single *Aat*II site to nucleotide 5604 (3′ primer carrying an *Xba*I site following a STOP codon). For

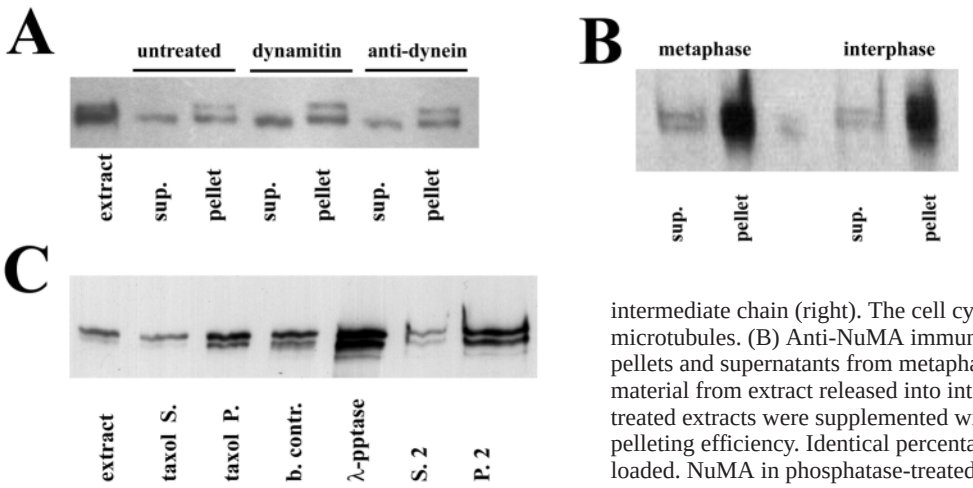

Fig. 1. Taxol-stabilized microtubules bind to NuMA from *Xenopus* egg extracts, irrespective of dynactin or dynein inhibition. (A) Anti-NuMA immunoblot of egg extract, and of supernatants (sup.) and pellets from extracts containing taxol-stabilized microtubules. Extracts were either untreated (left), or treated with recombinant dynamitin (middle), or monoclonal antibody against dynein intermediate chain (right). The cell cycle does not affect binding of NuMA to microtubules. (B) Anti-NuMA immunoblot; comparison of taxol microtubule pellets and supernatants from metaphase-arrested egg extract with equivalent material from extract released into interphase by calcium chloride. The taxol-treated extracts were supplemented with additional microtubules to increase the pelleting efficiency. Identical percentages of supernatants and pellets were loaded. NuMA in phosphatase-treated extract still binds to microtubules. (C) Anti-NuMA immunoblot of egg extract (extract), supernatant (taxol S.) and pellet (taxol P.) after centrifugation of taxol-treated extract, and the same pellet treated with either control buffer (b.contr.) or lambda phosphatase (λ-pptase). The phosphatase treatment consistently led to an increased immunoreactivity of NuMA on western blots (identical amounts were loaded for phosphatase treatment and controls, as verified by Ponceau staining in multiple experiments). The phosphatase-treated pellet was subsequently resuspended and re-centrifuged. The resulting supernatant (S.2) and pellet (P.2) are shown.

NuMAΔtailIIA+NLS, two PCR products were used: the first extended from the *Aat*II site to position 5598 (3′ primer carrying a *Bgl*II site), the second extended from nucleotide 5932 (5′ primer carrying a *Bgl*II site) to 6306 (3′ primer carrying an *Xba*I site following the endogenous STOP codon). The introduction of *Bgl*II did not modify the amino acid sequence at the deletion point. For both deletion constructs, the PCR products were first cloned into pBluescriptKS NuMA using *Aat*II/*Xba*I, then transferred into pCDNA3 GFP-NuMA using *Eco*RV/*Xba*I. An overview of the various constructs is given in Fig. 3E.

Expression levels of GFP NuMA constructs were measured by trypsinising and counting transfected HeLa cells from a culture dish, and analysing the levels of GFP signal by quantitative immunoblotting of HeLa extract, using a GFP-specific antibody, a ^{125}I-labelled secondary antibody, and a phosphoimager. Measured amounts of recombinant GFP were loaded on the same gel for calibration. The percentage of transfected cells was analysed by fluorescence microscopy of a glass coverslip with cells grown from the same culture dish, and the variation of NuMA levels was measured with a digital CCD camera (Zeiss Axiocam, Oberkochen, Germany) and Adobe PhotoShop software (Adobe, San Jose, CA).

Secondary structure prediction of NuMA tail IIA was conducted using PredictProtein software (Rost et al., 1994).

Results

NuMA binding to microtubules does not require dynein or dynactin

Previous work has shown that NuMA associates with the microtubule motor complex of dynein and its activator dynactin and that it moves towards spindle poles during mitosis (Merdes et al., 1996; Merdes et al., 2000). Moreover, accumulation of NuMA on the microtubule minus ends was partially inhibited by antibodies against dynein, or addition of excess amounts of dynamitin, the p50 subunit of the dynactin complex. However, despite inhibition of dynein or dynactin, substantial amounts of NuMA were still bound along the surface of spindle microtubules, suggesting that binding of NuMA to the spindle and transport towards the pole are two distinct events. To test this possibility in a biochemical approach, we re-designed the experiment in metaphase-arrested cytoplasmic extract capable of forming asters from taxol-stabilized microtubules (Gaglio et al., 1995; Gaglio et al., 1996; Gaglio et al., 1997). Pelleting of this material from *Xenopus* egg extracts revealed that more than 50% of NuMA binds to the taxol-stabilized microtubules, irrespective of whether dynein or dynactin are inhibited or not (Fig. 1A). In the same experiment, we detected an enrichment of a slower migrating form of NuMA in the pellets, raising the question whether post-translationally modified NuMA in metaphase extracts or alternatively a splice variant (Tang et al., 1994) might possess a higher binding affinity to microtubules. Because NuMA has been reported to be phosphorylated during mitosis (Sparks et al., 1995; Gaglio et al., 1995; Compton and Luo, 1995), we tested whether conversion of metaphase-arrested extract into interphase extract by the addition of calcium chloride and loss of cdc2 kinase activity (Murray, 1991) affected the binding properties of NuMA (Fig. 1B). Generation of interphase extract did not alter the migration of the NuMA doublet, even though a sample of the same extract, to which frog sperm was added, disassembled all mitotic spindles and re-formed interphase nuclei (data not shown). Extracts containing nuclei were able to drive NuMA import into the nucleoplasm (Merdes et al., 1996); however, the small number of nuclei was unable to segregate all NuMA from the large volume of extract. Therefore, the majority of NuMA remained cytoplasmic and was able to interact with microtubules. Moreover, NuMA in both metaphase extract and interphase extract pelleted with taxol-stabilized microtubules to the same degree, indicating that cell cycle has no significant effect on NuMA binding to microtubules. In further experiments, we tested whether treatment of taxol-microtubule pellets from extracts with lambda phosphatase affected the microtubule binding of NuMA, but couldn't detect a significant difference in co-pelleting between the phosphatased fast migrating form of NuMA and the slow migrating form after

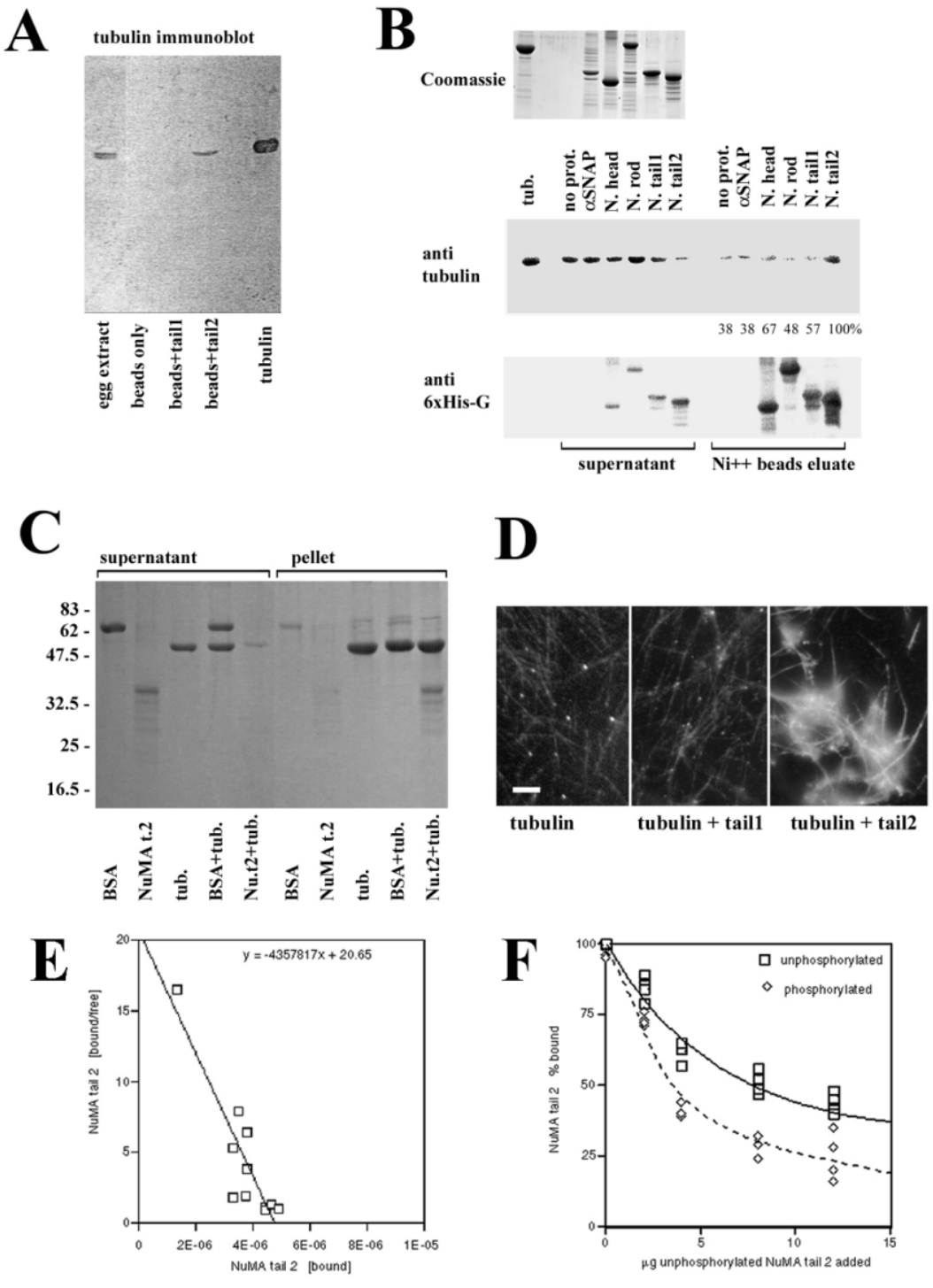

Fig. 2. A region within the distal half of the NuMA tail domain binds directly to tubulin. (A) Immunoblot for tubulin, showing *Xenopus* egg extract, and eluates of Ni-agarose beads after incubation in untreated egg extract (beads only), or egg extract supplemented with hexa-histidine-tagged *Xenopus* NuMA tail I (beads+tail1) or NuMA tail II (beads+tail2). For comparison, phosphocellulose-purified tubulin (tubulin) is shown. (B) Top: Coomassie-stained gel showing purified tubulin (tub.), hexa-histidine tagged αSNAP (αSNAP), and hexa-histidine-tagged fusion proteins of *Xenopus* NuMA head domain (N. head), a 425-residue fragment of the *Xenopus* NuMA rod domain (N. rod), the proximal half of the *Xenopus* NuMA tail (N. tail1), and the distal half of the *Xenopus* NuMA tail (N. tail2). Middle: immunoblot for tubulin, showing a binding assay of soluble tubulin mixed with hexa-histidine-tagged fusion proteins as shown on the Coomassie-stained gel, and adsorbed to magnetic Ni-agarose beads. Supernatants (left) and bead eluates (Ni++ beads eluate, right) are shown. 'no prot.' indicates a control of soluble tubulin, binding to Ni-beads only; 'tub.' indicates purified tubulin only. The relative amounts of tubulin bound in each reaction were measured with a phosphoimager and noted underneath; the NuMA tail2 sample, showing the strongest binding, was set to 100%. Bottom: an identical immunoblot, probed with antibody against the peptide sequence of hexa-His-Gly (anti 6×His-G). The lack of reactivity against the αSNAP fusion protein is due to cloning in a pQE-9 vector, encoding hexa-histidine without glycine. All other fusion proteins were cloned in pRSET, leading to immunoreactive fusion proteins containing hexa-His-Gly. (C) Coomassie stained gel, showing supernatants and pellets of bovine serum albumin (BSA), *Xenopus* NuMA tail II (NuMA t.2), taxol-stabilized microtubules (tub.), and taxol-stabilized microtubules incubated with bovine serum albumin (BSA+tub.) or *Xenopus* NuMA tail II (Nu.t2+tub.). (D) Microtubule assembly from phosphocellulose-purified tubulin mixed with rhodamine-labelled tubulin, without additions (left), or with added *Xenopus* NuMA tail I (middle), or tail II (right). Bar, 20 µm. (E) Scatchard plot, showing *Xenopus* NuMA tail II binding at increasing concentrations (in mol/l) to taxol-stabilized microtubules. (F) The percentage of bound *Xenopus* NuMA tail II to taxol-stabilized microtubules, quantifying unphosphorylated protein (open squares), or γ counts of NuMA tail II phosphorylated with recombinant cdc2 kinase/cyclinB and radioactive ATP (open diamonds).

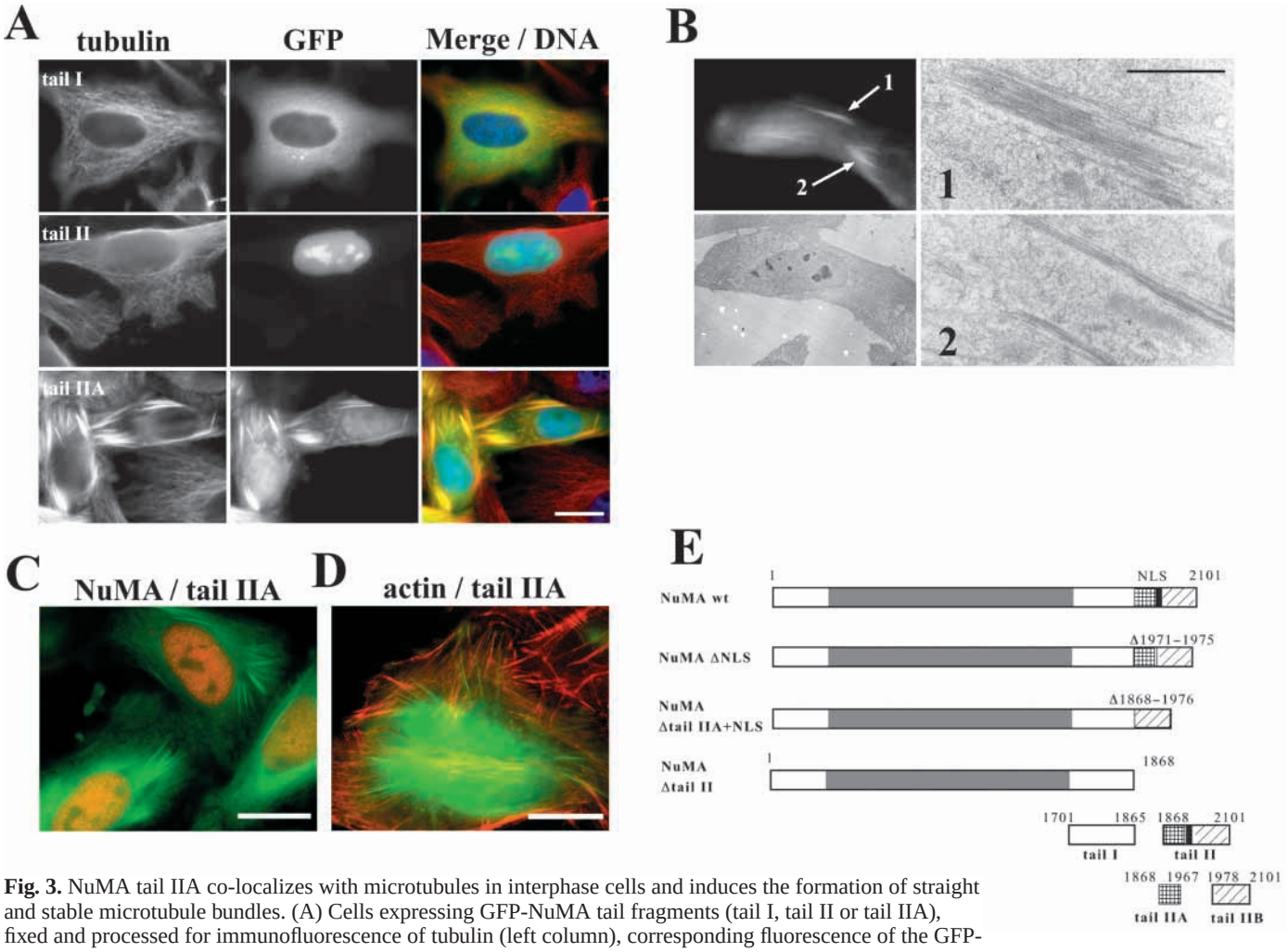

Fig. 3. NuMA tail IIA co-localizes with microtubules in interphase cells and induces the formation of straight and stable microtubule bundles. (A) Cells expressing GFP-NuMA tail fragments (tail I, tail II or tail IIA), fixed and processed for immunofluorescence of tubulin (left column), corresponding fluorescence of the GFP-tag (middle column), and merged fluorescence (right column). Red, tubulin; green, GFP; blue, chromosomes stained with DAPI. Bar, 20 μm. (B) Cell expressing GFP-NuMA tail IIA, fixed and processed for fluorescence microscopy of GFP (upper left panel), followed by electron microscopy. Lower left panel: low magnification electron micrograph of the same cell, upper and lower right panels: high magnification views showing microtubule bundles in areas 1 and 2, as indicated by arrows in the GFP fluorescence micrograph. Bar, 1 μm. (C,D) Cells expressing GFP-NuMA tail IIA (green), fixed and processed for immunofluorescence of endogenous NuMA (C, red), or fluorescence of actin using rhodamine-phalloidin (D, red). Bars, 20 μm (C,D). (E) Diagram of the various human NuMA constructs used for transfection experiments. Amino acid positions are indicated.

solubilisation and re-pelleting (Fig. 1C). Our data indicate that NuMA possesses an affinity for microtubules independent of its dynein/dynactin transporter or the cell cycle.

NuMA binds directly to tubulin

To test the possibility of a direct NuMA-tubulin interaction, we purified bacterial fusion proteins covering the various domains of *Xenopus* NuMA and assayed their binding to tubulin. NuMA has a tripartite structure, comprising a central α-helical rod domain flanked by globular head and tail domains. Because previous reports pointed towards an interaction between spindle microtubules and the tail domain of NuMA (Compton and Cleveland, 1993; Maekawa and Kuriyama, 1993; Tang et al., 1994; Gueth-Hallonet et al., 1996), we studied whether tubulin could be isolated from *Xenopus* egg extracts by affinity interaction with hexa-histidine tagged fusion proteins of the first and second half of the NuMA tail domain (tail I and tail II, respectively) (Merdes et al., 1996). As shown in Fig. 2A, only the distal half of the NuMA tail (tail II) was able to bind to tubulin. To determine whether other regions of the NuMA molecule possessed any affinity to tubulin, we also purified fusion proteins of the head domain, as well as a 425 amino acid long region within the rod domain, and αSNAP as a control protein, usually involved in membrane vesicle fusion. All proteins were incubated with soluble pure tubulin, and isolated using magnetic nickel agarose beads. Fig. 2B shows that the tail II region of NuMA has the highest affinity to tubulin. A relatively high background binding of tubulin to beads alone complicated this experiment. In a different assay, NuMA tail II fusion protein bound quantitatively to taxol-stabilized microtubules (Fig. 2C). This experiment also demonstrated that the amount of soluble tubulin left in the supernatant was significantly reduced after NuMA tail II incubation compared with controls incubating with BSA or no additional protein. We used this assay to incubate taxol-stabilized microtubules with

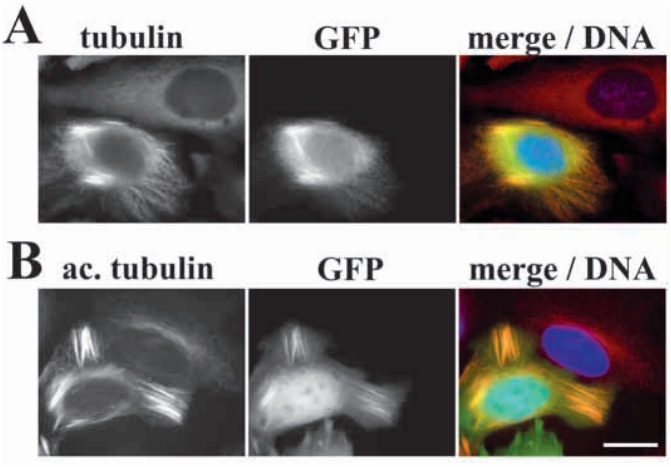

Fig. 4. NuMA tail IIA stabilises microtubules. Cells expressing GFP-NuMA tail IIA (green) were incubated on ice for 1 hour, fixed and processed for immunofluorescence of tubulin (A, red) or incubated at room temperature and stained for acetylated tubulin (B, red). Chromosomes are stained with DAPI (blue). Note the absence of a microtubule network in the untransfected cell in (A) Bar, 20 μm.

increasing concentrations of NuMA tail II, to estimate the binding constant under saturating conditions. Scatchard plot analysis (Fig. 2E) revealed an affinity constant K_A of 4×10^6 M^{-1} (±2), which is in good agreement with values previously published for microtubule associated proteins (Andersen et al., 1994; Butner and Kirschner, 1991). Because putative cdc2 kinase phosphorylation sites had been reported in the NuMA tail (Compton and Luo, 1995), we tested the microtubule-binding properties of NuMA tail II treated with recombinant cdc2/cyclinB protein. NuMA tail II was efficiently phosphorylated using [γ-^{32}P]ATP (not shown), and was pelleted with taxol-stabilized microtubules in a competition assay, at increasing concentrations of unphosphorylated NuMA. Consistent with our data on equal microtubule binding by interphase or metaphase NuMA (see above), this assay revealed that phosphorylation by cdc2 kinase did not increase NuMA binding (Fig. 2F), but led to a small reduction of the microtubule affinity compared with unphosphorylated NuMA tail II. This reduction was only about 1.6-fold and sometimes within the variance of the experiment. The NuMA tail II fragment also had a striking morphological effect on microtubule organization: when polymerized from phosphocellulose purified tubulin, thick cables of microtubules formed in the presence of NuMA tail II (Fig. 2D), each containing parallel bundles of multiple microtubules, as shown previously by electron microscopy (Merdes et al., 1996).

A 100-residue region in the NuMA tail induces stable microtubule bundles in vivo

The observation of microtubule bundles in vitro led us to investigate whether NuMA tail II had a similar effect on microtubule organization in the living cell. A tagged form of human NuMA tail II, containing GFP at its N-terminus, was overexpressed and followed by fluorescence microscopy in HeLa cells. In interphase, the fusion protein segregated entirely into the nucleus (Fig. 3A), due to its nuclear localization signal between amino acids 1970 and 1991 [corresponding to positions 1984 and 2005 in a longer NuMA isoform (see Tang et al., 1994; Gueth-Hallonet et al., 1996)]. However, when NuMA tail II was further truncated to remove the nuclear localization signal and all C-terminal amino acids (Fig. 3E), the resulting construct tail IIA decorated multiple thick fibres in the cytoplasm of interphase cells (Fig. 3A). These fibres represented parallel bundles of microtubules, as shown both by immunofluorescence microscopy and electron microscopy (Fig. 3A,B). To test whether tail II also aligned alongside actin-containing stress fibres, we performed staining with phalloidin and demonstrated that NuMA tail IIA and actin bundles did not co-localize (Fig. 3D). We showed that the formation of microtubule bundles was a direct effect of the NuMA tail IIA expression and not mediated by endogenous full-length NuMA, which localized entirely to the nucleus and was not present in the cytoplasmic fibres (Fig. 3C). In this experiment, endogenous NuMA was detected with the rod-specific antibody 1F1 (Compton et al., 1991), which does not crossreact with the NuMA tail IIA construct. Other regions of NuMA such as the distal half of the tail (tail I) had no effect on microtubule organization (Fig. 3A). Also, further truncation of tail IIA did not produce any fusion proteins capable of microtubule binding (data not shown), suggesting that tail IIA defines the minimal domain necessary for microtubule binding and bundling.

The microtubule bundles formed in the presence of NuMA tail IIA were unusually stable and resisted prolonged cold treatment (Fig. 4A). Consistent with this, the bundles stained positively with an antibody against acetylated tubulin (Fig. 4B), a previously characterized marker for stable microtubule arrays (Webster and Borisy, 1989).

We measured the expression levels of GFP NuMA tail IIA causing this phenotype by quantitative immunoblotting and by fluorescence microscopy, and determined a range between 0.1 and 1 pg protein per cell, equivalent to 2-20 million copies per cell. This range is between 10 and 100 times more than the number of copies of endogenous NuMA per cell (Compton et al., 1992). We found that the strongest effects on microtubule bundling were obtained above 0.3 pg GFP NuMA tail IIA per cell.

The NuMA tail IIA fragment induces abnormal spindle poles

In mitosis, the 100-residue region of NuMA tail IIA caused the formation of abnormal spindle poles when overexpressed. A variety of phenotypes was observed: in 47% of the cells (n=150), additional spindle poles were observed (Fig. 5A) that also contained endogenous, full length NuMA (Fig. 5B); in 27% of the cells, bipolar spindles formed with one of two poles being unusually large, and with mono-oriented chromosome pairs grouped around the larger pole; in 14% of the cells, virtually no pole separation could be seen, resulting in astral microtubule arrays with rosettes of mono-oriented chromosomes. Only 12% of the cells overexpressing tail IIA displayed apparently normal bipolar spindles. Identical phenotypes were seen when the longer, 234-residue construct tail II was overexpressed. The formation of asymmetric spindles with enlarged polar microtubule asters or additional poles was reminiscent of mitotic cells treated with taxol-related

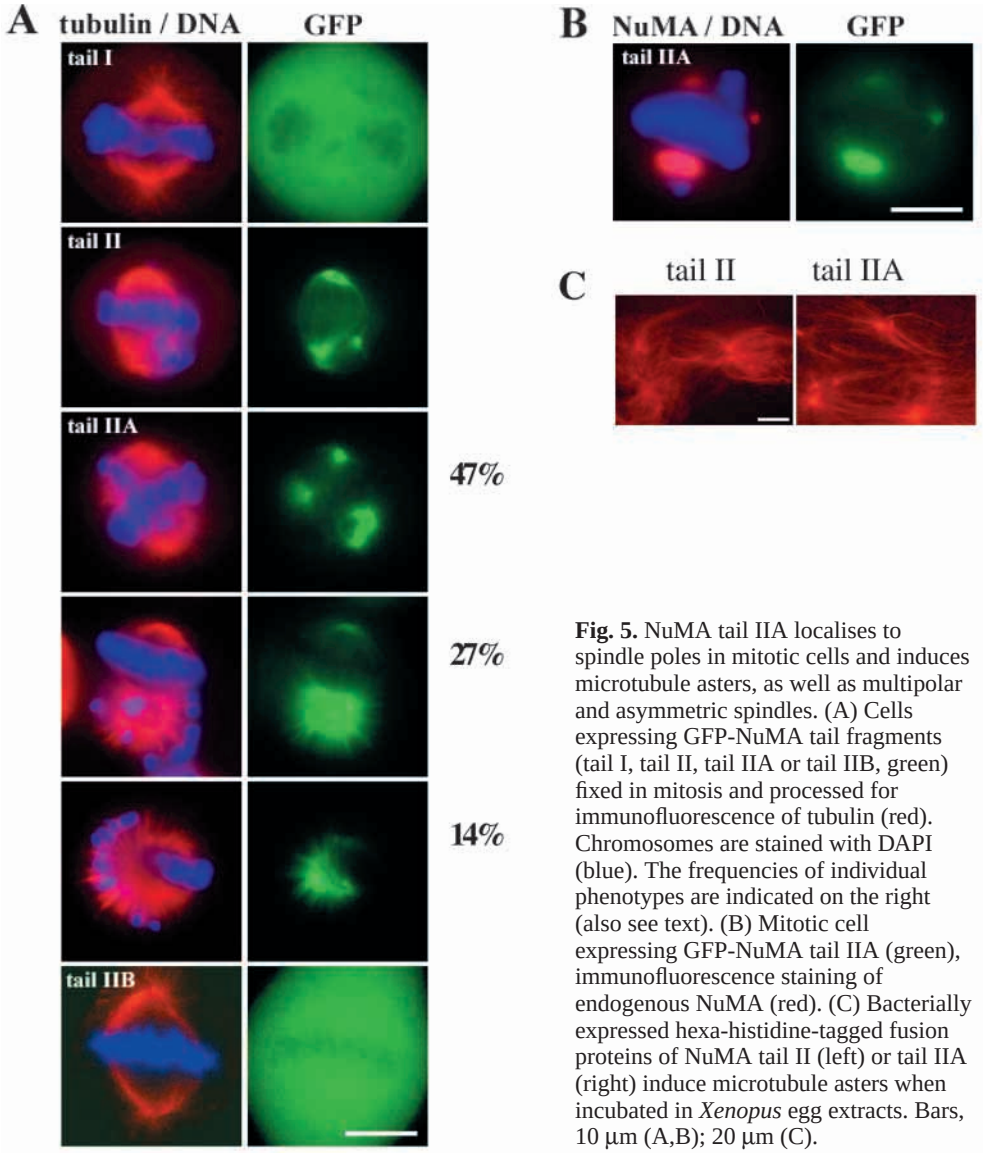

Fig. 5. NuMA tail IIA localises to spindle poles in mitotic cells and induces microtubule asters, as well as multipolar and asymmetric spindles. (A) Cells expressing GFP-NuMA tail fragments (tail I, tail II, tail IIA or tail IIB, green) fixed in mitosis and processed for immunofluorescence of tubulin (red). Chromosomes are stained with DAPI (blue). The frequencies of individual phenotypes are indicated on the right (also see text). (B) Mitotic cell expressing GFP-NuMA tail IIA (green), immunofluorescence staining of endogenous NuMA (red). (C) Bacterially expressed hexa-histidine-tagged fusion proteins of NuMA tail II (left) or tail IIA (right) induce microtubule asters when incubated in *Xenopus* egg extracts. Bars, 10 μm (A,B); 20 μm (C).

drugs (Paoletti et al., 1997). As with taxol, this effect of tail IIA may be explained by local microtubule stabilization. Similar to previous findings with bacterially expressed NuMA tail II (Merdes et al., 1996), the shorter fusion protein of NuMA tail IIA was able to induce large microtubule asters when added to metaphase *Xenopus* egg extracts (Fig. 5C). Any tail fragments lacking the 100 amino acids of tail II, such as tail I or tail IIB, localized diffusely in metaphase cells, without effects on spindle pole organization or any other aspects of cell division (Fig. 5A).

Without tail IIA, NuMA can no longer bind to microtubules by itself

Whereas full-length wild-type NuMA concentrates quantitatively in the nucleus (Fig. 3C), mutant NuMA in which the nuclear localization sequence has been rendered unfunctional, accumulates in the cytoplasm and has a severe effect on microtubule organization. In previous studies (Saredi et al., 1996; Gueth-Hallonet et al., 1996; Gueth-Hallonet et al., 1998), such mutant protein was seen in cytoplasmic aggregates with a fibrous substructure and co-localized with large amounts of aggregated tubulin polymers. In a similar experiment in this report, tubulin aggregates were induced by full-length NuMA in which the nuclear localization signal was deleted (Fig. 6A, top row), but did not form when the tubulin binding region was deleted. Both deletion of the entire tail II region at the C-terminus (Δtail II), as well as specific removal of the nuclear localization sequence plus the 100-residue region of tail IIA (Δtail IIA+NLS) produced NuMA molecules that failed to concentrate tubulin during interphase (Fig. 6A, middle and bottom rows). However, in mitosis, both mutant forms of NuMA were still able to bind to the spindle and to concentrate at the poles (Fig. 6B), presumably by interaction with endogenous full-length NuMA.

Discussion

We have shown that NuMA can interact with microtubules by direct binding to tubulin. Using purified components in vitro, we have mapped the tubulin binding site to the distal half of the NuMA tail domain (NuMA tail II) and, in a series of transfection experiments, we have further narrowed down the binding site to amino acids 1868-1967 of human NuMA (tail IIA). The fact that a GFP fusion protein is targeted to interphase microtubules by tail IIA, and that a deletion mutant of NuMA lacking tail IIA and the nuclear localization signal fails to interact with tubulin, indicates that the tail IIA region is both necessary and sufficient for tubulin binding. The finding that the same NuMA mutants, lacking the tubulin binding site, still bind to mitotic spindle poles appears to contradict this hypothesis. However, in contrast to interphase cells, endogenous NuMA is now freed into the mitotic cytoplasm and able to bind to the deletion mutant via its dimer-forming rod domain (Harborth et al., 1995) and therefore contribute to the spindle targeting of the mutant protein. Our findings are consistent with reports in which C-terminal deletion mutants of NuMA after amino acid residue 1936 were able to induce tubulin aggregates, whereas truncation after residue 1921 abolished this effect. (Note that in Gueth-Hallonet's work, deletion mutants were numbered Δ1950 and Δ1935, because they were made from a NuMA isoform that contains 14 additional amino acids in the rod domain.) The truncation after amino acid 1921 must have eliminated essential sequence

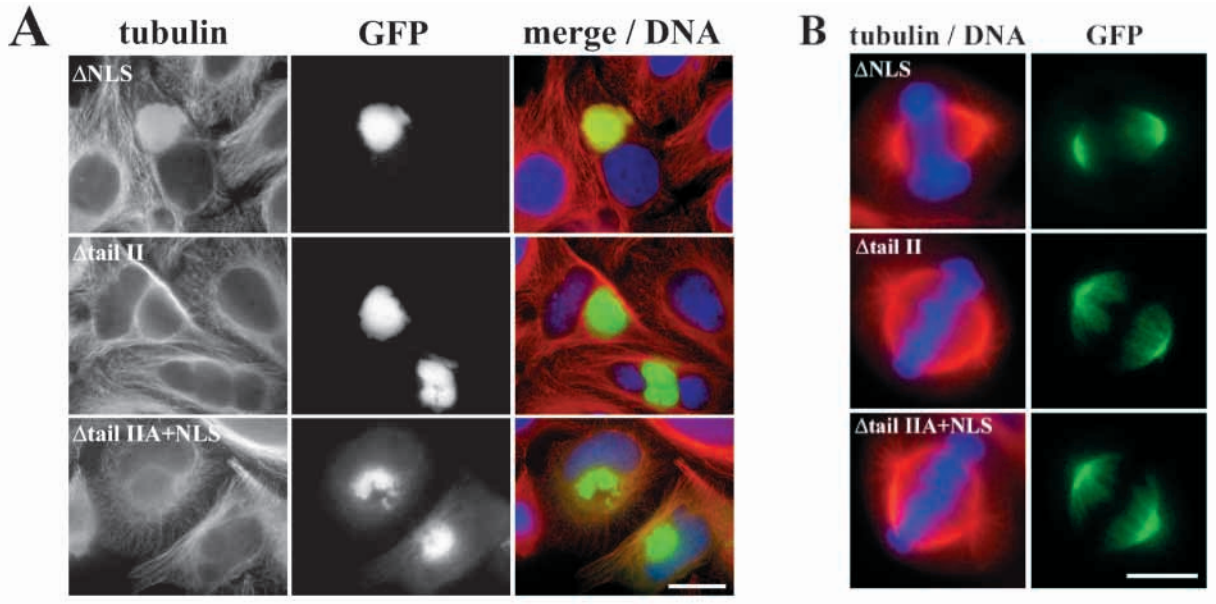

Fig. 6. Full-length NuMA requires tail IIA to associate with tubulin when expressed in the cytoplasm of interphase cells. Cells expressing GFP-NuMA ΔNLS, Δtail II or Δtail IIA+NLS (green), fixed and processed for immunofluorescence of tubulin (red). Chromosomes are stained with DAPI (blue). (A) Interphase cells. Note the presence of tubulin aggregates co-localizing with GFP-NuMA ΔNLS (top row), and the absence of tubulin in protein aggregates of the mutants lacking tail II or tail IIA. Bar, 20 μm. (B) Mitotic cells. Bar, 10 μm.

within the tail IIA region. Based on these results, one might conclude that the tubulin binding region is restricted to sequence from amino acids 1868 to 1936. We tested whether this smaller region was still able to target a GFP fusion protein to microtubules, but failed to see any association (not shown). One possible explanation would be that, to fold properly, the tubulin binding region needs flanking sequence either at the N-terminus or the C-terminus, and that such flanking sequence would be lost in a fusion protein that is too small. The predicted secondary structure of this region includes two short α-helices flanking a loop of 23 amino acids, with high sequence conservation in human and *Xenopus* NuMA (67% identity). The 100 amino acid region characterized in this work shows microtubule binding affinity similar to that of other microtubule-associated proteins, but doesn't carry sequence similarities with any known MAP. Whereas proteins of the MAP2/tau family and MAP4 contain up to four repeats of a conserved 31 amino acid sequence mediating microtubule binding (Lewis et al., 1988; West et al., 1991; Doll et al., 1993), and MAP 1B contains several repeats of the sequence KKEE, KKEI or KKEV (Noble et al., 1989), no repeats are found within the microtubule binding site of NuMA. Moreover, the amino acid composition of the microtubule binding motif in NuMA is significantly different from other MAPs: the tau sequence in rat contains 23% basic amino acids in its microtubule binding site, bringing the calculated isoelectric point of this domain to 10.3. This is similar in MAP2 and MAP 4, whereas NuMA contains a more acidic microtubule binding site with an amino acid composition of only 12% basic amino acids in human, or 14% in *Xenopus* NuMA, and an isoelectric point of 5.1 or 5.6, respectively.

A surprising finding was that NuMA tail IIA not only decorated microtubules along their length, but also massively induced the formation of strong microtubule bundles, both in cells and in microtubule polymerization assays in vitro (see also Merdes et al., 1996). The induction of bundles could be explained either by the existence of multiple tubulin binding sites within the 100 amino acid region of NuMA tail IIA, or by the ability of multiple NuMA tail IIA polypeptides to bind each other. According to the first model, this small region would have to contain two tubulin binding sites, separated by sufficient linker sequence to bridge two adjacent microtubules. The second scenario seems more likely: NuMA has been shown to form large fibrous networks (Saredi et al., 1996; Gueth-Hallonet et al., 1998; Harborth et al., 1999) that are based on dimerization of the NuMA rod domains and on the subsequent association of multiple NuMA dimers via their tail domains. Harborth et al. reported that the binding of multiple NuMA tail domains to each other does not depend on the last 112 amino acids of the tail, indicating that oligomerization is largely mediated by tail I or tail IIA (Harborth et al., 1999). Thus, the binding of multiple tail IIA polypeptides to each other could well mediate the association of parallel microtubules. Moreover, the formation of spindle poles during cell division could be explained in two steps: first, the polar accumulation of NuMA driven by dynein/dynactin (Merdes et al., 2000) and, second, the direct binding of the NuMA tail domain to the microtubule surface, whereby networks of multiple NuMA dimers linked at their tail domains would maintain a focussed array of spindle fibres. The binding of NuMA to the microtubule surface could provide an additional step of regulating spindle dynamics by preventing uncontrolled disassembly of microtubule minus ends and by increasing the stability of the mitotic apparatus, as shown by our finding that NuMA tail IIA increases microtubule stability.

It is still unclear which mechanisms regulate NuMA binding to the spindle and what causes the release of NuMA from the microtubule ends and its re-import into nuclei during

telophase. Phosphorylation of NuMA by cdc2/cyclin B has been suggested to affect binding to spindle microtubules (Compton and Luo, 1995; Gaglio et al., 1995). We have tested this possibility directly by phosphorylating NuMA tail II in vitro with cdc2 kinase, but could not detect major differences in microtubule binding affinity. Although there is no doubt that full length NuMA is phosphorylated during mitosis (Sparks et al., 1995; Gaglio et al., 1995; Compton and Luo, 1995), details on the regulation through specific kinases still remain to be investigated. It is possible that a large protein such as NuMA, with multiple potential phosphorylation sites in various domains, is regulated by more than one kinase. Furthermore, the regulation of NuMA binding to microtubules might involve additional factors and might not be directly affected by phosphorylation. Given that overexpressed NuMA tail IIA as well as full-length NuMA in frog egg extracts can bind avidly to microtubules both in interphase and mitosis, participation of other factors seems to be the most likely explanation. One recently suggested mechanism involves the regulation by importin β and Ran GTP (Wiese et al., 2001; Nachury et al., 2001). Recent reports showed that the tail II region of NuMA can bind and focus microtubules into mitotic asters after an inhibitor, importin β, is released from NuMA by Ran GTP. Consequently, at the exit of mitosis, NuMA could re-associate with importin β, detach from the spindle and subsequently get transported into the nucleus. Using our microtubule pelleting assay, we tested whether importin α or β prevented NuMA tail II binding to microtubules, but were unable to detect any effect (A.M., unpublished). During the course of this study, another binding partner of NuMA, the protein LGN, has been identified and its interaction domain characterized (Du et al., 2001): LGN binds to NuMA amino acids 1818-1930, which largely overlap with the microtubule binding site. Most interestingly, LGN seems to negatively regulate the interaction between NuMA and microtubule asters and might therefore be an important factor during mitotic spindle organization. Of course, the mechanisms that regulate microtubule aster formation in vivo might be far more complex, and other components in addition to importin α, β, LGN and NuMA are currently being identified (Gruss et al., 2001). Based on the present work, we propose that NuMA can organize microtubules by a direct interaction, and that the segregation of NuMA into the nucleus after mitosis is necessary to prevent interference with the microtubule network.

We thank Anne Paton and Fiona Gardiner for their help with the expression of fusion proteins, Xavier Fant for cloning GFP-tagged NuMA tail I, Alexander Dammermann and Xavier Fant for critically reading the manuscript, and all our colleagues for helpful suggestions. We thank Duane Compton (Dartmouth Medical School, Hanover, NH) for the gift of pUC19 NuMAΔNLS, Paul McLaughlin, Ken Sawin, and Catherine Rabouille (University of Edinburgh, Scotland) for the gift of labelled phalloidin, recombinant GFP, and αSNAP plasmid, respectively. This work was supported by a Wellcome Trust Senior Research Fellowship to A.M.

References

Andersen, S. S., Buendia, B., Dominguez, J. E., Sawyer, A. and Karsenti, E. (1994). Effect on microtubule dynamics of XMAP230, a microtubule-associated protein present in *Xenopus* laevis eggs and dividing cells. *J. Cell Biol.* **127**, 1289-1299.

Avides, M. C. and Glover, D. M. (1999). Abnormal spindle protein, Asp, and the integrity of mitotic centrosomal microtubule organizing centers. *Science* **283**, 1733-1735.

Butner, K. A. and Kirschner, M. W. (1991). Tau protein binds to microtubules through a flexible array of distributed weak sites. *J. Cell Biol.* **115**, 717-730.

Charrasse, S., Schroeder, M., Gauthier-Rouviere, C., Ango, F., Cassimeris, L., Gard, D. L and Larroque, C. (1998). The TOGp protein is a new human microtubule-associated protein homologous to the *Xenopus* XMAP215. *J. Cell Sci.* **111**, 1371-1383.

Compton, D. A. (1998). Focusing on spindle poles. *J. Cell Sci.* **111**, 1477-1481.

Compton, D. A. and Cleveland, D. W. (1993). NuMA is required for the proper completion of mitosis. *J. Cell Biol.* **120**, 947-957.

Compton, D. A. and Luo, C. (1995). Mutations in the predicted p34cdc2 phosphorylation sites in NuMA impair the assembly of the mitotic spindle and block mitosis. *J. Cell Sci.* **108**, 621-633.

Compton, D. A., Yen, T. J. and Cleveland, D. W. (1991). Identification of novel centromere/kinetochore-associated proteins using monoclonal antibodies generated against human mitotic chromosome scaffolds. *J. Cell Biol.* **112**, 1083-1097.

Compton, D. A., Szilak, I. and Cleveland, D. W. (1992). Primary structure of NuMA, an intranuclear protein that defines a novel pathway for segregation of proteins at mitosis. *J. Cell Biol.* **116**, 1395-1408.

Cullen, C. F. and Ohkura, H. (2001). Msps protein is localized to acentrosomal poles to ensure bipolarity of *Drosophila* meitotic spindles. *Nat. Cell Biol.* **3**, 637-642.

Cullen, C. F., Deak, P., Glover, D. M. and Ohkura, H. (1999). Mini spindles: a gene encoding a conserved microtubule associated protein required for the integrity of the mitotic spindle in *Drosophila*. *J. Cell Biol.* **146**, 1005-1018.

Dionne, M. A., Sanchez, A. and Compton, D. A. (2000). ch-TOGp is required for microtubule aster formation in a mammalian mitotic extract. *J. Biol. Chem.* **275**, 12346-12352.

Doll, T., Meichsner, M., Riederer, B. M., Honegger, P. and Matus, A. (1993). An isoform of microtubule-associated protein 2 (MAP2) containing four repeats of the tubulin-binding motif. *J. Cell Sci.* **106**, 633-640.

Du, Q., Stukenberg, P. T. and Macara, I. G. (2001). A mammalian partner of inscuteable binds NuMA and regulates mitotic spindle organization. *Nat. Cell Biol.* **3**, 1069-1075.

Gaglio, T., Saredi, A. and Compton, D. A. (1995). NuMA is required for the organization of microtubules into aster-like arrays. *J. Cell Biol.* **131**, 693-708.

Gaglio, T., Saredi, A., Bingham, J. B., Hasbani, M. J., Gill, S. R., Schroer, T. A. and Compton, D. A. (1996). Opposing motor activities are required for the organization of the mammalian mitotic spindle pole. *J. Cell Biol.* **135**, 399-414.

Gaglio, T., Dionne, M. A. and Compton, D. A. (1997). Mitotic spindle poles are organized by structural and motor proteins in addition to centrosomes. *J. Cell Biol.* **138**, 1055-1066.

Gergely, F., Karlsson, C., Still, I., Cowell, J., Kilmartin, J. and Raff, J. W. (2000a). The TACC domain identifies a family of centrosomal proteins that can interact with microtubules. *Proc. Natl. Acad. Sci. USA* **97**,14352-14357.

Gergely, F., Kidd, D., Jeffers, K., Wakefield, J. G. and Raff, J. W. (2000b). D-TACC: a novel centrosomal protein required for normal spindle function in the early *Drosophila* embryo. *EMBO J.* **19**, 241-252.

Gruss, O. J., Carazo-Salas, R. E., Schatz, C. A., Guarguaglini, G., Kast, J., Wilm, M., Le Bot, N., Vernos, I., Karsenti, E. and Mattaj, I. W. (2001). Ran induces spindle assembly by reversing the inhibitory effect of importin alpha on TPX2 activity. *Cell* **104**, 83-93.

Gueth-Hallonet, C., Weber, K. and Osborn, M. (1996). NuMA: a bipartite nuclear location signal and other functional properties of the tail domain. *Exp. Cell Res.* **225**, 207-218.

Gueth-Hallonet, C., Wang, J., Harborth, J., Weber, K. and Osborn, M. (1998). Induction of a regular nuclear lattice by overexpression of NuMA. *Exp. Cell Res.* **243**, 434-452.

Harborth, J., Weber, K. and Osborn, M. (1995). Epitope mapping and direct visualization of the parallel, in-register arrangement of the double-stranded coiled-coil in the NuMA protein. *EMBO J.* **14**, 2447-2460.

Harborth, J., Wang, J., Gueth-Hallonet, C., Weber, K. and Osborn, M. (1999). Self assembly of NuMA: multiarm oligomers as structural units of a nuclear lattice. *EMBO J.* **18**, 1689-1700.

Kuriyama, R., Kofron, M., Essner, R., Kato, T., Dragas-Granoic, S., Omoto, C. K. and Khodjakov, A. (1995). Characterization of a minus end-directed kinesin-like motor protein from cultured mammalian cells. *J. Cell Biol.* **129**, 1049-1059.

Lee, M. J., Gergely, F., Jeffers, K., Peak-Chew, S. Y. and Raff, J. W. (2001). Msps/XMAP215 interacts with the centrosomal protein D-TACC to regulate microtubule behaviour. *Nat. Cell Biol.* **3**, 643-649.

Lewis, S. A., Wang, D. and Cowan, N. (1988). Microtubule-associated protein MAP2 shares a microtubule binding motif with tau protein. *Science* **242**, 936-939.

Maekawa, T. and Kuriyama, R. (1993). Primary structure and microtubule-interacting domain of the SP-H antigen: a mitotic map located at the spindle pole and characterized as a homologous protein to NuMA. *J. Cell Sci.* **105**, 589-600.

Matthies, H. J. G., McDonald, H. B., Goldstein, L. S. B. and Theurkauf, W. B. (1996). Anastral spindle morphogenesis: role of the non-claret disjunctional kinesin-like protein. *J. Cell Biol.* **134**, 455-464.

Merdes, A. and Cleveland, D. W. (1997). Pathways of spindle pole formation: different mechanisms; conserved components. *J. Cell Biol.* **138**, 953-956.

Merdes, A., Ramyar, K., Vechio, J. D. and Cleveland, D. W. (1996). A complex of NuMA and cytoplasmic dynein is essential for mitotic spindle assembly. *Cell* **87**, 447-458.

Merdes, A., Heald, R., Samejima, K., Earnshaw, W. C. and Cleveland, D. W. (2000). Formation of spindle poles by dyein/dynactin-dependent transport of NuMA. *J. Cell Biol.* **149**, 851-861.

Mountain, V., Simerly, C., Howard, L., Ando, A., Schatten, G. and Compton, D. A. (1999). The kinesin-related protein, HSET, opposes the activity of Eg5 and cross-links microtubules in the mammalian mitotic spindle. *J. Cell Biol.* **147**, 351-366.

Murray, A. W. (1991). Cell cycle extracts. In *Methods in Cell Biology*, Vol. 36 (ed. B. K. Kay and H. B. Peng), pp. 581-605. San Diego: Academic Press.

Nachury, M. V., Maresca, T. J., Salmon, W. C., Waterman-Storer, C. M., Heald, R. and Weis, K. (2001). Importin beta is a mitotic target of the small GTPase Ran in spindle assembly. *Cell* **104**, 95-106.

Noble, M., Lewis, S. A. and Cowan, N. J. (1989). The microtubule binding domain of microtubule-associated protein MAP1B contains a repeated sequence motif unrelated to that of MAP2 and tau. *J. Cell Biol.* **109**, 3367-3376.

Paoletti, A., Giocanti, N., Favaudon, V. and Bornens, M. (1997). Pulse treatment of interphasic HeLa cells with nanomolar doses of docetaxel affects centrosome organization and leads to catastrophic exit of mitosis. *J. Cell Sci.* **110**, 2403-2415.

Rost, B., Sander, C. and Schneider, R. (1994). PHD – an automatic mail server for protein secondary structure prediction. *Comput. Appl. Biosci.* **10**, 53-60.

Saredi, A., Howard, L. and Compton, D. A. (1996). NuMA assembles into an extensive filamentous structure when expressed in the cell cytoplasm. *J. Cell Sci.* **109**, 619-630.

Sparks, C. A., Fey, E. G., Vidair, C. A. and Doxsey, S. J. (1995). Phosphorylation of NuMA occurs during nuclear envelope breakdown and not mitotic spindle assembly. *J. Cell Sci.* **108**, 3389-3396.

Tang, T. K., Tang, C. C., Chao, Y. J. and Wu, C. W. (1994). Nuclear mitotic apparatus protein (NuMA): spindle association, nuclear targeting and differential subcellular localization of various NuMA isoforms. *J. Cell Sci.* **107**, 1389-1402.

Wakefield, J. G., Bonaccorsi, S. and Gatti, M. (2001). The *Drosophila* protein Asp is involved in microtubule organization during spindle formation and cytokinesis. *J. Cell Biol.* **153**, 637-648.

Webster, D. R. and Borisy, G. G. (1989). Microtubules are acetylated in domains that turn over slowly. *J. Cell Sci.* **92**, 57-65.

West, R. R., Tenbarge, K. M. and Olmsted, J. B. (1991). A model for microtubule-associated protein 4 structure. *J. Biol. Chem.* **266**, 21886-21896.

Wiese, C., Wilde, A., Moore, M. S., Adam, S. A., Merdes, A. and Zheng, Y. (2001). Role of importin-β in coupling Ran to downstream targets in microtubule assembly. *Science* **291**, 653-656.

Whiteheart, S. W., Griff, I. C., Brunner, M., Clary, D. O., Mayer, T., Buhrow, S. A. and Rothman, J. E. (1993). SNAP family of NSF attachment proteins includes a brain-specific isoform. *Nature* **362**, 353-355.

Wittmann, T., Wilm, M., Karsenti, E. and Vernos, I. (2000). TPX2, a novel *Xenopus* MAP involved in spindle pole organization. *J. Cell Biol.* **149**, 1405-1418.

Yang, C. H., Lambie, E. J. and Snyder, M. (1992). NuMA: an unusually long coiled-coil related protein in the mammalian nucleus. *J. Cell Biol.* **116**, 1303-1317.